JOURNAL OF Applied Polymer SCIENCE

Superhydrophobic surfaces with silane-treated diatomaceous earth/resin systems

Helanka J. Perera,[1] Bal K. Khatiwada,[1,2] Abhijit Paul,[1,3] Hamid Mortazavian,[1] Frank D. Blum[1]

[1]Department of Chemistry, Oklahoma State University, Stillwater, Oklahoma, 74078

[2]Department of Chemistry, University of the Ozarks, Clarksville, Arkansas, 72830

[3]Polymer Science and Engineering Department, Conte Center for Polymer Research, 120 Governors Drive, University of Massachusetts, Amherst, Massachusetts, 01003

Correspondence to: F. D. Blum (E-mail: fblum@okstate.edu)

ABSTRACT: Superhydrophobic coatings were prepared using fluorosilane-treated diatomaceous earth (DE) with either polyurethane or epoxy binders. The surface wettability and morphology of the films were analyzed using contact angle measurements and scanning electron microscopy (SEM), respectively. The water contact angles were studied as a function of the fluorocarbon fraction on DE and the particle loadings of treated DE in the coating. The contact angles exceeded 150° for coatings with at least 0.02 fluorocarbon fraction (mass of fluorosilane/mass of particle) on the DE and with 0.2 particle loadings (mass of treated particles/mass of coating). The water contact angles of the surfaces were dependent on the nature of the binder below 0.2 particle loadings of the superhydrophobic DE particles, but were independent of the binder type after attaining superhydrophobicity. The results were consistent with the superhydrophobicity resulting from the migration of the superhydrophobic DE moving to and covering the surfaces completely. It was also shown that the treatment with fluorosilanes restricted the pores in DE and reduces the specific surface area of the material. However, these changes had effectively no effect on the superhydrophobicity of the coatings. The results of this work clearly identify some important considerations relative to producing superhydrophobic coatings from inexpensive diatomaceous earth. © 2016 Wiley Periodicals, Inc. J. Appl. Polym. Sci. **2016**, *133*, 44072.

KEYWORDS: coatings; epoxy; polyurethanes; resins; surfaces and interfaces

Received 12 March 2016; accepted 9 June 2016

DOI: 10.1002/app.44072

INTRODUCTION

Diatoms are unicellular algae of the class of Bacillariophyceae of Phylum Bacilloriophyta.[1] Diatoms extract silicon from water for the production of their exoskeletons, called frustules or hydrated silica shells.[2,3] When diatoms cells die, their tiny shells sink, and with time, these shells form layers of fossil deposits. These fossilized deposits are known as diatomaceous earth (DE) or kieselgur.[3,4] DE particle sizes can vary between 1 μm and several mm in diameter.[5,6] There are more than 100,000 different species with unique three-dimensional frameworks.[7] Each three-dimensional DE structure contains millions of microscopic, hollow, perforated cylindrical, and disk shaped shells. The resulting DE is an inert, highly porous, lightweight, and thermally resistant material.[5,8] Naturally occurring DE is hydrophilic; consequently, it can be used in applications as adsorbents,[4,9] in filtration,[10–14] and in construction materials as a filler.[15] Chemically modified, DE has been used in additional applications, such as materials for superhydrophobic coatings,[6,16–18] metal adsorbents,[4] and drug delivery.[19–22]

Surfaces that form static water contact angles greater than 150° and have sliding angles less than 10° are defined as superhydrophobic surfaces.[23–27] The superhydrophobicity of a solid surface is determined by two factors: its chemical composition and micro-nano hierarchical texture.[23–25,28] Modifying a surface with low energy chemical groups can effectively increase the water contact angle of a solid surface. Surfaces with CF_2 and CF_3 groups generally have low surface energies with contact angles of about 120° on a flat surface.[29,30] Roughening the surface can result in contact angles as high as 160 to 175°, and the surfaces become non-wettable.[31,32] These superhydrophobic coatings are water-repellent, self-cleaning, and can be used in many applications, such as anti-icing, anti-oxidation, anti-fogging, non-wetting, buoyancy, and flow enhancement.[33–35]

There are many ways to fabricate superhydrophobic surfaces; they include plasma etching,[36–38] graft-on-graft polymerization,[39] chemical vapor deposition,[40] lithography,[41] sol–gel processing,[42] and self-assembly of low surface energy materials. However, most of the methods used to fabricate superhydrophobic surfaces are

complicated, expensive, cannot be used on a large scale, or require special apparatus. Therefore, developing a facile and inexpensive approach for obtaining superhydrophobic surfaces is important. The use of a low-cost material such as diatomaceous earth particles is obviously worth consideration.

Our objective was to produce superhydrophobic coatings using fluorosilane-treated diatomaceous earth particles (DE) with polymer binders that are inexpensive and have low volatile organic contents. DE has already been made into superhydrophobic particles through a variety of novel chemistries.[6,16–18] Puretskiy, *et al.*[6] showed that a hydrophobic polymer could be grafted-from DE to make superhydrophobic anti-icing materials. Sticking the particles to the top of epoxy coatings provided improved the mechanical properties of the DE layer. However, the multistep process is multi-step complicated. Simpson *et al.*,[43] Oliveria *et al.*,[16] and Polizos *et al.*[17] have shown that fluorosilanes grafted to DE could make superhydrophobic DE particles. Coatings with treated DE and polydimethylsiloxane can be improved with the inclusion of graphene oxide.[18] While these studies showed that superhydrophobic coatings could be made using very specific formulations, little has been reported about some of the basic parameters, which affect the particles, and the behavior and structures of the coatings produced from them.

To produce more effective coatings, additional efforts to understand the basic behavior of the coatings systems were undertaken. For example, the effects on the superhydrophobicity of coatings systems on either the amount grafted fluorocarbons on DE or the particle loadings of treated DE in the coatings are not well known. In addition, the roles of different binder systems have not been a focus of reported work. In this study, we report contact angle measurements, scanning electron microscopy, specific surface areas of particles, and pore size measurements to understand the development of superhydrophobicity and to characterize the surface properties of the coatings produced.

EXPERIMENTAL

Treated diatomaceous earth (FS-DE) samples with different amounts of fluorosilane treatments were obtained from Dry Surface Coatings, (Guthrie, OK). Bisphenol A based epoxy resin (Epon 828) with an epoxy equivalent of 185–192 g was provided by Exel Logistics, (Houston, TX). A cycloaliphatic amine curing agent (Ancamine 2280) with an amine equivalnt weight of 110 g was supplied by Air Products and Chemicals (Allentown, PA). An aliphatic polyisocyanate resin based on hexamethylene diisocynate (Desmodur N75) with isocyanate (-NCO) content of $16.5 \pm 0.3\%$ and an equivalent weight average of 255 was obtained from Bayer MaterialScience, (Baytown, TX). An alkoxylated polyol curing agent (Polyol 3611) with hydroxyl number of 610 ± 25 was supplied by Innovadex, (Overland Park, KS), tetrahydrofuran (THF), and hexane were from Fisher Scientific (Pittsburgh, PA).

Two types of binder solutions were prepared: epoxy binders and polyurethane binders. The epoxy binder solutions were prepared by thoroughly mixing a stoichiometric amount of epoxy resin and curing agent in THF in a ratio of 0.32 g:1 mL. For the polyurethane binder solutions, polyisocyanate and polyol curing agent were prepared in a 1.05 to 1 molar ratio (the excess amount of polyisocyanate ensures complete reaction of the polyol and provides optimal film properties) and mixed with THF in a ratio of 1 g:1 mL. The binders were mixed in a mechanical shaker for 15 min to make a homogenous solution.

Two different sets of samples were prepared. The first set was a series of coatings made from treated DE samples with different amounts of fluorosilanes. The treated DE particles with different amounts of fluorosilane were then used to prepare epoxy coatings with a fixed 0.25 FS-DE particle loading. The particle loadings are shown as fractions of the mass of the DE (treated or untreated) to the mass of the DE plus polymer resin. In contrast, the fluorocarbon fractions on DE are given as the mass fractions of fluorocarbon (from thermogravimetric analysis, TGA) to the total mass of treated particles (DE plus fluorocarbon). The second set of samples was a series of epoxy and polyurethane coatings with a single kind of treated DE sample containing a fluorocarbon fraction of 0.036 (FS-DE-1). This fluorocarbon fraction was selected based on having a sufficient amount of fluorosilane for the samples to be superhydrophobic. Different particle loadings of FS-DE-1 were mixed with polymer binders. THF was then added to each vial to make the total volume constant. All the samples were mixed using a mechanical shaker for 30 min.

For contact angle measurements, the FS-DE polymer binder samples were coated on glass slides (7.5×2.5 cm^2) cleaned with toluene. Around 0.7 mL from each FS-DE polymer sample was applied onto a glass slide to yield a flat, thin, and uniform layer. The epoxy and polyurethane coated samples were kept on a flat surface to air dry and then placed in an oven at 180 °C for 20 min to cure.

Water contact angle measurements were performed using static sessile drop method at room temperature using a homebuilt contact angle measurement instrument with a high-resolution Proscope camera capable of recoding 15 fps at a 640×480 resolution. The contact angles were measured using Low Bond Axisymmetric Drop Shape Analysis (LB-ADSA) technique[44–46] by fitting the best profile to an image of 5-μL droplet of deionized water on the surface. The drop shape analysis was done using a drop analysis plugin with ImageJ software. Five readings from different locations on the surface were taken, averaged, and reported as the contact angle for each sample. The reproducibility of the contact angle values on five different places of the sample was less than $\pm 5°$ (one standard deviation).

The fluorocarbon fractions in the FS-DE were quantified by thermogravimetric analysis (TGA) using a Q-50 Thermogravimetric Analyzer (TA Instruments, New Castle, DE). The samples were heated from 20 to 950 °C at a heating rate of 20 °C/min under 40 mL/min of continuous airflow.

Nitrogen adsorption–desorption isotherms over a relative pressure range from 0.005 to 0.990 (P/P_0) were done with a NOVA 2200e instrument (Quantachrome Instruments, Boynton Beach, FL) at 77 K to measure the specific surface area and pore size

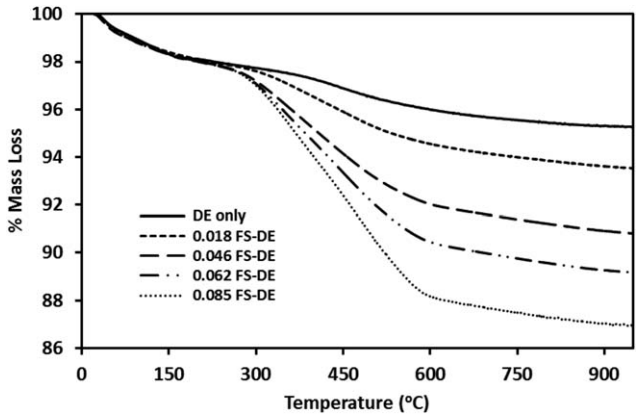

Figure 1. The TGA curves of untreated and treated DE (particles without polymer binder) with different fluorocarbon fractions. The labels are based on the fluorocarbon fractions, determined by the difference between the mass loss of each treated DE and the untreated DE sample at 950°C.

distribution of samples. Samples were outgassed at 50 °C for 3 h under a nitrogen stream prior to the analysis. Surface areas were calculated using at least five relative pressures within the range of linearity of the physical adsorption theory ($0.05 < P/Po < 0.35$) by applying the Brunauer-Emmet-Teller (BET)[47] equation. The pore size distributions were determined using the density functional theory (DFT) method.[48]

The surface features were characterized with scanning electron microscopy (SEM). For the SEM studies, aluminum pans with an inside diameter of 5 cm were coated with 2 mL of the dispersion. A small portion of the coatings (with the aluminum dish) was cut and attached to the top of an aluminum stub. Samples were then made conductive by sputtering with Au/Pd and imaged using an FEI Quanta 600 SEM (FEI Company, Hillsboro, OR).

RESULTS

The TGA thermograms for DE and FS-DE samples, shown in Figure 1, were used to determine the amount of grafted fluorosilane on the DE. The TGA curves showed that untreated DE had a mass loss fraction of around 0.026 at 950 °C. The fluorocarbon fraction was calculated using the difference between the mass loss of FS-DE and the mass loss of untreated DE samples at 950 °C. It has been shown for trialkoxysilanes undergoing thermal degradation that the alcohol groups were removed during hydrolysis and the hydrocarbon chains (fluorocarbon in this case) volatilized. The so called Q-species, with Si bonded to four oxygens, were shown to be the predominant Si species from the coupling agents, left on the particles after the chains degraded.[49] For simplicity, we report only the fluorocarbon fraction of fluorosilane, based only on the mass of fluorocarbon chains. As evident from Figure 1, the mass fractions of grafted fluorosilane for different samples were within the range of 0.009–0.085.

The effect of the amount of the fluorosilane on the water contact angle of treated DE particles was studied. The contact angles for epoxy films with 0.25 particle loading and different fluorocarbon fractions on DE particles are shown in Figure 2. Epoxy film with untreated DE had a contact angle of 115°. The hydrophobicity of the epoxy films was enhanced upon the addition of treated DE particles. The contact angle of the coatings increased with increased fluorocarbon fraction on the DE particles. When the fluorocarbon fraction on DE was around 0.02 (0.02 g of fluorosilane in 0.98 g of DE), the maximum hydrophobicity was obtained and the contact angles remained fairly constant with increased fluorocarbon fraction of fluorosilane up to 0.08. In other words, fluorocarbon fractions of 0.02 or more were enough to decrease the surface energy to provide superhydrophobicity, i.e., with water contact angles above 160°, in this case.

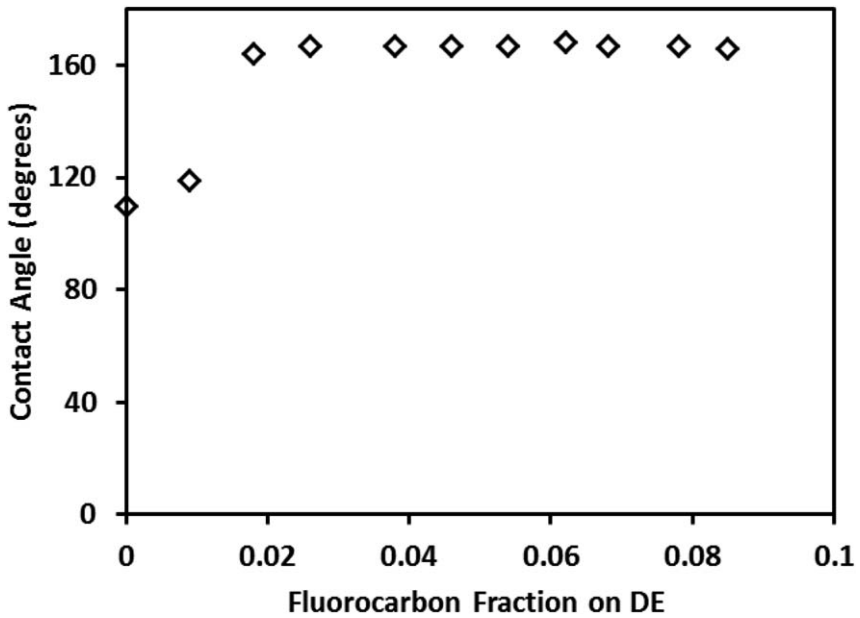

Figure 2. Contact angles of epoxy coatings as a function of the fluorocarbon fraction on DE for samples with 25% FS-DE particle loading. The coatings with fluorocarbon fractions above 0.02 were superhydrophobic and the contact angles were independent of the fluorocarbon fraction.

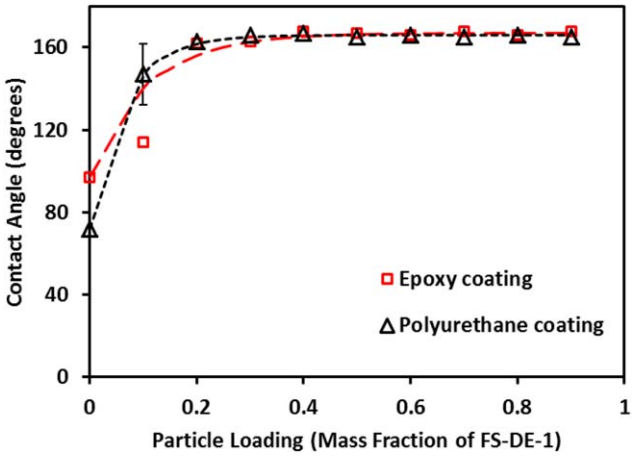

Figure 3. The contact angles of epoxy and polyurethane coatings as a function of the FS-DE-1 particle loading. Except for the error bar shown, the standard deviations of the uncertainties in the measurements were less than the size of the symbols for data points. The particles used contained 0.036 fluorocarbon fraction of fluorosilane. [Color figure can be viewed in the online issue, which is available at wileyonlinelibrary.com.]

The dependence of the contact angles of epoxy and polyurethane films on the treated DE particle loadings is shown in Figure 3. The treated DE particles contained a 0.036 fluorocarbon fraction. Bulk polyurethane and bulk epoxy had contact angles of 72° and 96°, respectively. These contact angle values were consistent with other studies.[50–53] Additional FS-DE particles caused the contact angles to increase, reaching superhydrophobicity with both epoxy and polyurethane after particle loadings of 0.2 of FS-DE. The treated DE particles migrated to the surface easily, likely due to the low viscosity of starting solutions. The ultimate superhydrophobicity after this mass fraction was independent of the starting contact angle of the polymer binder. At mass fractions of the FS-DE larger than 0.2, coatings with both polymer binders behaved similarly, suggesting that the wettability of the coatings might be dominated by the treated DE particles.

SEM images for untreated DE particles are shown in Figure 4. The majority of the particles were disk-shaped and a small fraction of them were cylindrical-shaped. The disk-shaped frustules, as shown in Figure 4(a), had typical diameters of 10–20 μm. The particles had highly developed macroporous (larger than 50 nm) structures with the pore diameter of around 250 to 300 nm, which are seen in Figure 4(b,c). As shown in Figure 4(c), each one of the macropores (about 200 nm) was included mesoporous (2–50 nm) structures with pore diameters in the range of 12–25 nm [Figure 4(d)]. The specific surface area of untreated DE was measured by us to be 24.1 ± 0.8 m^2/g, as was also found in previous studies.[4,54] Treated DE, with 0.046 and 0.085 fluorocarbon fractions of fluorosilane, were found to have specific surface areas of 17.0 ± 0.2 and 14.9 ± 0.6 m^2/g, respectively. These measurements show that the treatment of DE particles with fluorosilane reduces the specific surface area significantly.[4]

The presence of micro roughness was obvious from the SEM images. However, to further confirm the presence of nano size structure on DE particles, we studied the pore size distribution of these particles using the adsorption/desorption isotherms of nitrogen gas. The pore size distribution curves of treated and untreated DE are shown in Figure 5 and confirm that DE has primarily mesoporous structures with a pore diameter range of 2–35 nm with majority of them around 14 and 24 nm. The peaks maximum at 14 and 24 nm were likely due to the small pores shown in Figure 4(c), which shows pores in the range of 12–25 nm in the SEM. Upon the addition of 0.046 and 0.085 fluorocarbon fraction, the area under the pore size distribution decreased by 40 and 58%, respectively, relative to that of the untreated DE.

SEM images were taken from the coating-air interface of the films. Shown in Figure 6(a), the SEM images of the epoxy coating with no FS-DE show a relatively smooth film with no distinct features. With the addition of FS-DE, a rough topography was apparent on the smooth epoxy surface, which can be seen in Figure 6(b–f). At a particle loading of 0.12 FS-DE, as shown

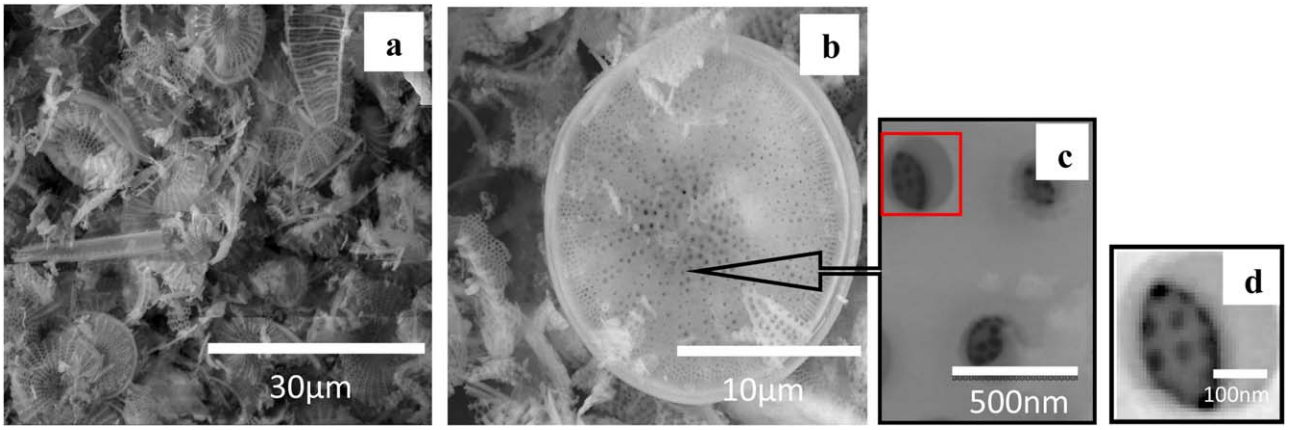

Figure 4. SEM images of untreated DE (a) scale bar 30 μm, (b) typical structure of a single disk-shaped untreated DE with scale bar of 10 μm, (c) macroporous (about 200 nm) and mesoporous (dark spots inside the holes, about 25 nm) structures of disk-shaped DE; scale bar 500 nm, and (d) enlarged macropore with scale bar of 100 nm. The SEM images show nano- and microscale roughness of DE particles. [Color figure can be viewed in the online issue, which is available at wileyonlinelibrary.com.]

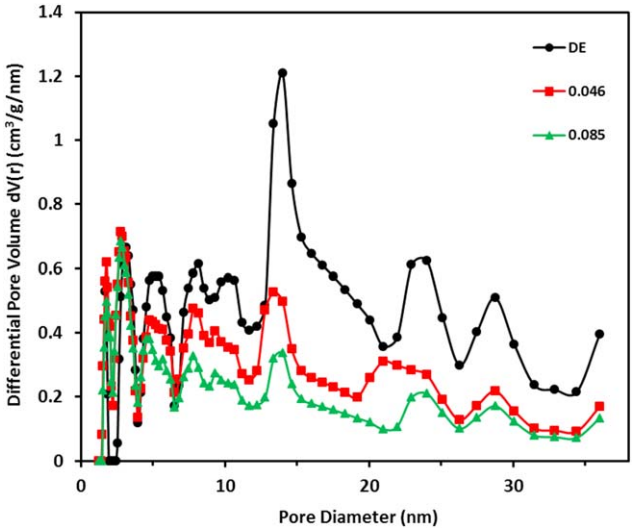

Figure 5. Pore size distribution of untreated DE and treated DE with fluorocarbon fractions of 0.046 and 0.085. Grafting with fluorosilane filled up some of the mesoporous structures of the DE. With increased grafted amounts of fluorosilane, more pores were filled. [Color figure can be viewed in the online issue, which is available at wileyonlinelibrary.com.]

in Figure 6(b), the surface shows some parts of FS-DE particles that were coated with the epoxy binder, as well as areas with just epoxy binder on the surface (darker smooth areas). When the particle loading of FS-DE was increased to 0.28, shown in Figure 6(c), the particles of DE became clearer with only small polymer regions. Both FS-DE partially covered and fully exposed particles occurred at the surface. At a particle loading of 0.34 FS-DE, Figure 6(d), the surface looked similar to that of the fraction of 0.28 with partially polymer binder covered particles of FS-DE on the surface. The SEM micrographs for the samples with additional FS-DE are shown in Figure 6(e–f). There were no noticeable changes in the micrographs of these FS-DE coatings. They all consisted of large amounts of FS-DE particles on top of the coatings with no significant amount of polymer binder apparent.

The SEM images of the polyurethane coatings with different particle loading amounts of FS-DE are shown in Figure 7(a–f). As can be seen in Figure 7(a), the surface of the polyurethane binder coating was smooth and featureless, similar to the epoxy binder without FS-DE. SEM images of the polyurethane coatings with different mass fractions of FS-DE particles were mostly consistent with those of the epoxy coatings. At a mass fraction of 0.11, the surface in Figure 7(b), most of the FS-DE particles that appeared on the surface were polyurethane resin coated. There were also areas with just polymer on the surface. As the mass fraction of FS-DE was increased, the surfaces seemed fully coated with FS-DE particles. Although the particles came to the surface, particles were still bound to the surface through the polymer binder in both the polyurethane and epoxy coatings. Particles were not dislodged from the surface by touch and the contact angles remained unchanged after 50 abrading cycles. The surface structure remained constant after about 0.20 mass fraction of FS-DE as shown in Figure 7(c–f). Only at a fraction of FS-DE particle loadings less than 0.2, did the surface show a noticeable amount of the polyurethane binder.

DISCUSSION

Treated and untreated DE in the TGA thermograms showed two mass loss steps. The first decomposition step took place around 0–250 °C, attributed to the removal of physically adsorbed water from the surface of the treated and untreated DE particles.[55,56] The second mass loss occurred around 250–950 °C, and corresponded to the dehydroxylation of silanol groups of DE for of untreated DE.[55,56] In treated DE samples, this second mass loss was a combination of both dehydroxylation of silanol groups and degradation of fluorocarbon chains.[57,58] The main difference between the treated and untreated DE was the mass of grafted fluorocarbon. As Figure 1 shows, the degradation of fluorocarbon chains had a significant broad mass loss; likely due to the amorphous nature of the grafted fluorocarbon.[59]

Previous studies have shown the absence or presence of the fluorosilanes on the surface through the use of X-ray photoelectron spectroscopy (XPS).[16,17] The F_{1S} region of the XPS spectrum was also indicative of the presence of several different CF species and in conjunction with other atomic species, namely Si, C, and O, was used for a surface elemental analysis. In addition, the use of energy dispersive X-ray (EDX) showed that the distribution of F on the particles was uniform. Similar to this report, the presence of the fluorosilane on the DE was responsible for the superhydrophobicity of the particles, and in our case, the coatings.

The surface energies of materials have direct effect on the water contact angle on the surfaces. The results of contact angle measurements as a function of the fluorocarbon fraction, shown in Figure 2, indicate that FS-DE was much more hydrophobic than DE. As is known, DE consists primarily, but not exclusively, of hydrated amorphous silica ($SiO_2 \cdot nH_2O$).[5,17] Therefore, the DE surface is rich in hydrophilic silanol groups and can be considered hydrophilic.[19] Treating the surface of DE with fluorosilane decreases the number of free silanol groups and at the same time, the surface is treated with a low surface-energy material.[17,60] As a result, the contact angle of an FS-DE treated surface was larger than that of an untreated DE surface. With an increasing fraction of grafted fluorosilane, more of the surface was covered with low surface energy superhydrophobic material. The presence of the treated DE at the surface resulted in larger contact angles for the coating surfaces. The minimum fluorocarbon fraction grafted to DE (at least for 0.25 particle loading), to achieve a superhydrophobic surface with a contact angle above 160° was 0.02. Larger amounts of fluorosilane grafted to the particles did not change the hydrophobicity of the surface.

Epoxy and polyurethane binders behaved similarly with different treated DE particle loadings when the surface was superhydrophobic and covered with treated particles. The bulk polyurethane showed a smaller water contact angle than bulk epoxy, as shown in Figure 3. This difference was due to the differences in the structures of the two bulk polymers. Polyurethane is more polar and more hydrophilic than epoxy resin.

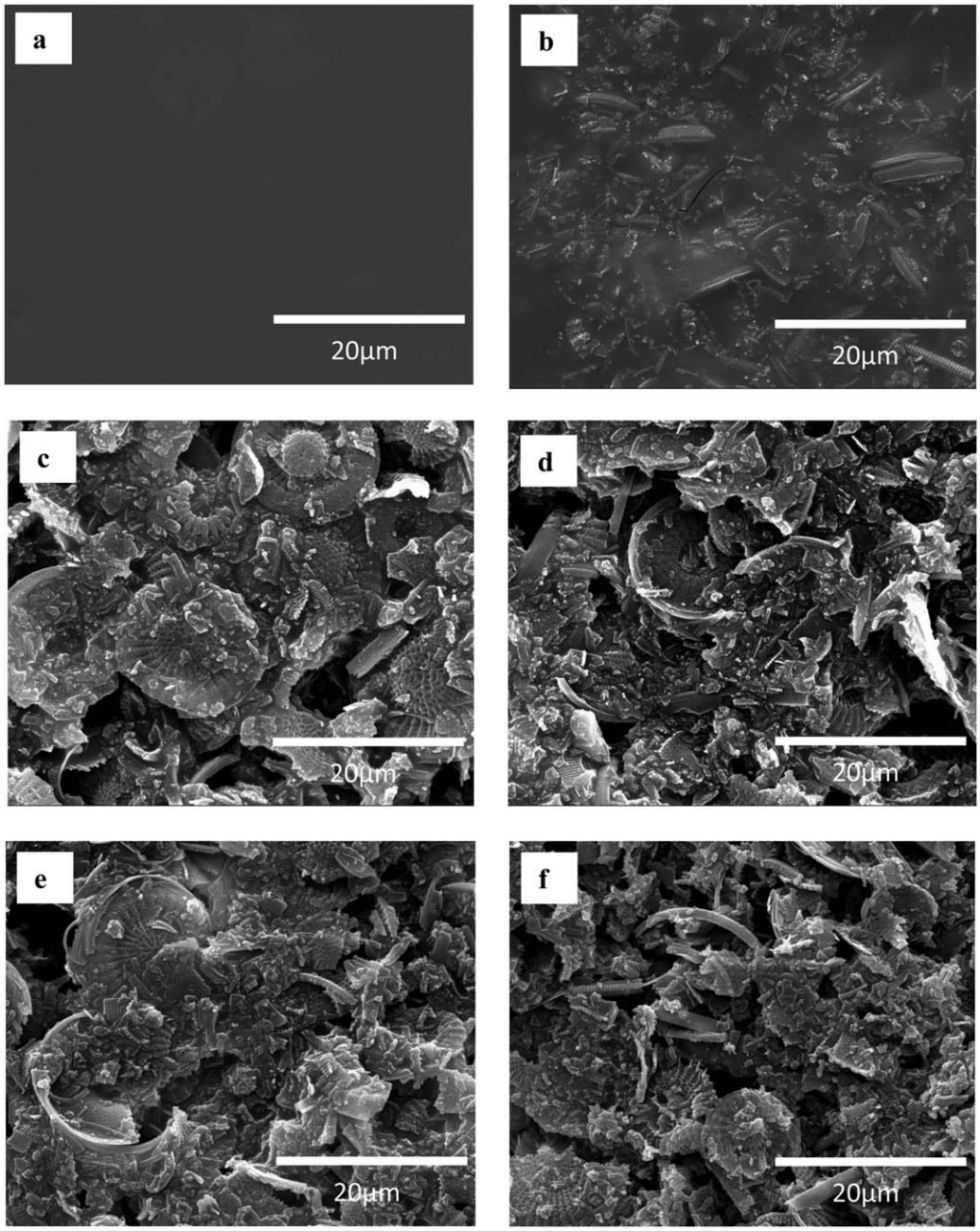

Figure 6. SEM images of epoxy coatings with different particle loadings of FS-DE (a) epoxy binder, (b) 0.12, (c) 0.28, (d) 0.34, (e) 0.40, and (f) 0.54 particle loadings of FS-DE. There was no significant change in the surface morphology of the samples with particle loadings of FS-DE greater than 0.28. The scale bar is 20 μm for each micrograph.

However, either of these polymers can be used as binders to make hydrophobic or superhydrophobic materials through the addition of treated DE particles. At particle loadings of 0.2 or greater, the similarity in the superhydrophobic range was because the surface became covered with treated particles. Apparently, the addition of more particles to the surface covers gaps between the particles and reduces the overall air trapped beneath the particles.[61,62]

When FS-DE was mixed with either polymer binder at sufficient particle loading, DE migrated to the surface and produced surface roughness,[16] with the fluorosilane providing the low energy surface. The combination of these two properties (surface roughness and low surface energy material) caused contact angles to increase.[63] With additional loadings of treated DE particles, the contact angles reached superhydrophobic levels with as little as 0.2 FS-DE particle loading. With the addition of more than 0.2 FS-DE particle loading in the coatings, the contact angles reached a plateau and remained around 160° without any significant changes.

It is clear that for our treated DE coatings to be superhydrophobic, the superhydrophobic DE particles need to cover the surface. The fluorination of the particles with silanes makes

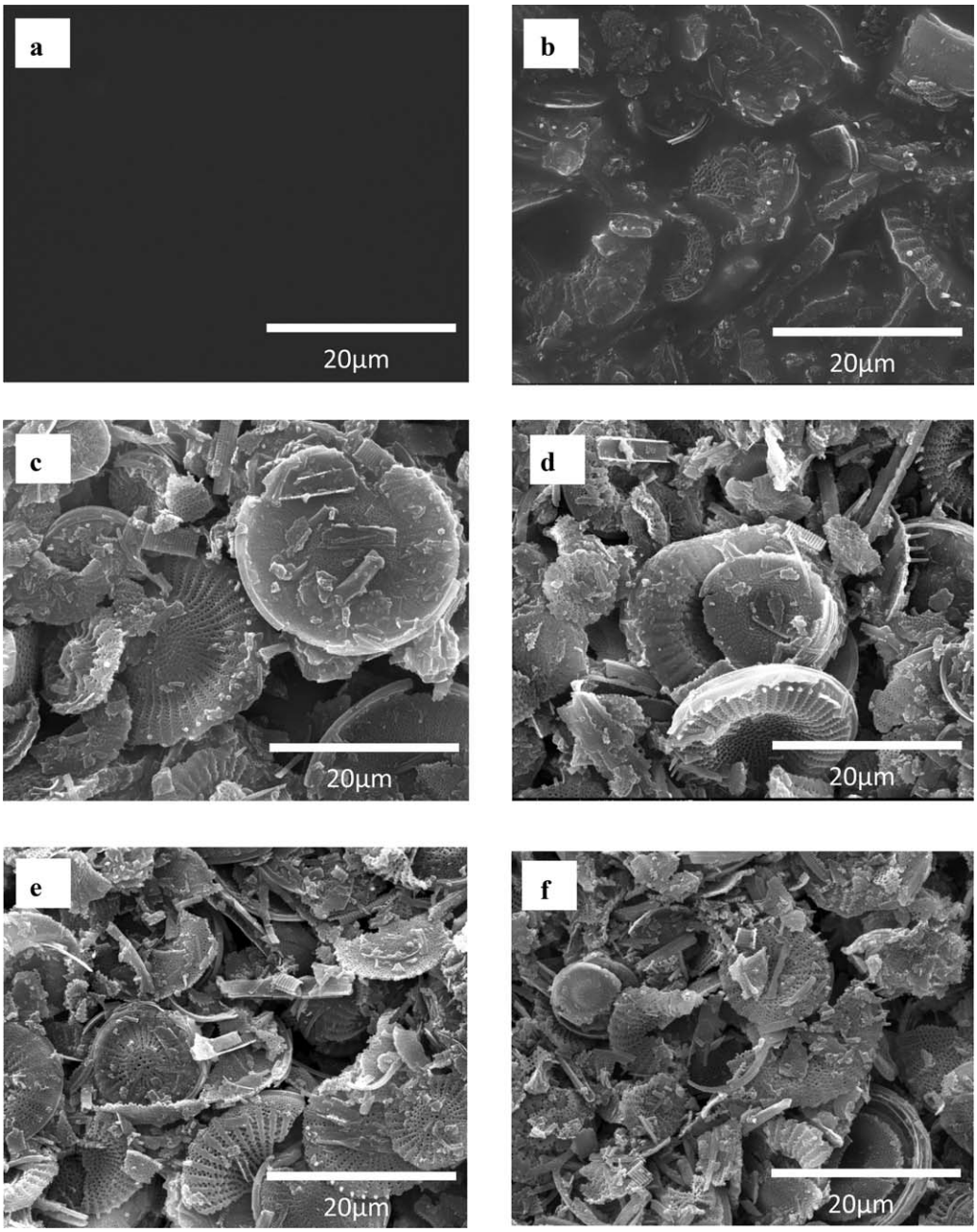

Figure 7. SEM images of polyurethane coatings with different particle loadings of FS-DE (a) Polyurethane binder, (b) 0.11, (c) 0.27, (d) 0.33, (e) 0.38, and (f) 0.53 (mass fraction particle loadings of FS-DE). The scale bar is 20 μm for each micrograph.

them somewhat incompatible with the solvent/monomer systems, so that some of the particles move to the air interface. The transport to the surface should depend on the local concentration of particles and the viscosity of the medium. The production of the epoxy and polyurethane coatings used here are based on low molecular mass monomers, so that the initial viscosities are lower than what would be expected for other systems, such as a preformed high molecular mass polymer. This low viscosity is the likely reason why the particle loadings were as small as 0.2 (w/w) for superhydrophobicity. For systems with larger viscosities, it takes larger particle loadings to achieve superhydrophobicity.

The porous nature of DE particles played an important role in the formation of specific surface area and roughness of the particles used. The DE skeletons from different sources have unique shapes, such as disk, triangular, funneled, and spiny. From Figure 4, SEM micrographs of untreated DE showed that the DE samples used by us were mostly composed of disk shaped particles with diameters of 10–20 μm. A small portion of the particles in the sample were cylindrically shaped with diameters less than 2 μm. The SEM results indicated that the DE particles have both nano- and micro-scale roughness, which are necessary for superhydrophobic surfaces,[64,65] resulting in macro- and mesopores. We estimate that the contribution of mesopores to

the surface area of untreated DE was four times larger than that from the macropores, which is in a good agreement with previous studies.[13,66] The pore size distribution results suggested that the majority of mesopores of DE were in the range of 12 to 30 nm, in agreement with the SEM results. The pore size distribution intensities decreased 40% for treated DE with 0.046 fluorocarbon fraction. This effect also seems to have resulted in a 30% reduction in specific surface area of the treated sample. Increasing the amount of fluorosilane to 0.085 fluorocarbon fraction of DE, reduced both porosity and specific surface area of treated samples further. The area under the pore size distribution and the specific surface area decreased 58% and 38%, respectively, compared to those of untreated DE. This result suggested that the fluorosilane either clogged or constricted the mesopores of the DE particles. Nevertheless, the macro- and mesoporosity sufficient for superhydrophobicity was retained.

The wettability of the coatings prepared with the treated DE particles depended on the amount of treated DE that migrated to the surface of the coatings. The epoxy and polyurethane coatings surfaces with small particle loadings had a mixture of the polymer binder and a small amount of FS-DE particles. In these samples, the surfaces did not have the suitable roughness and low surface energy necessary to be superhydrophobic. The correlation of the contact angle measurements and SEM micrographs was very strong. With particle loadings greater than 0.20 of FS-DE, sufficient numbers of particles were able to come to the surface providing the necessary surface roughness to be superhydrophobic.

CONCLUSIONS

A simple process has been developed to produce superhydrophobic coatings based on fluorocarbon-treated DE. This material holds promise for producing superhydrophobic coatings with water contact angles around 160°. The measurements made allow insight into the formation of superhydrophobic coatings, including a simple pathway, and the requirements (minimum fluorocarbon content, minimum particle loading, and transport of the particles to the surface) to produce superhydrophobic coatings with relatively inexpensive ingredients.

The amount of fluorocarbon (fluorocarbon fraction) required on the surface of the particles for superhydrophobicity with either polyurethane or epoxy coatings was 0.02 (mass of fluorocarbon/mass of particle). A minimum particle loading of treated-DE was determined to be about 0.2 for superhydrophobic coatings. At compositions greater than these two critical amounts, the nature of the resin system, polyurethane vs. epoxy, did not affect the water contact angles of the coatings. The reason for the resin independence of the coatings in the superhydrophobic range, was that the some of the fluorosilane-treated superhydrophobic particles escaped the low-viscosity resin mixture to reside at the air interface where they remained in the cured coating. For superhydrophobicity, the surfaces of the coatings were particle covered, as shown by SEM, with little or no exposed polymer. The fluorosilane treatments reduced the specific surface area of the particles and reduced their pore volumes, but these effects did not affect the superhydrophobicity. The surface roughness from the DE particles remained sufficient for superhydrophobicity.

ACKNOWLEDGMENTS

The authors thank Dry Surface Coatings, Guthrie, OK for supplying the raw materials for this work and helpful discussions about the particles used.

REFERENCES

1. Vrieling, E. G.; Beelen, T. P. M.; van Santen, R. A.; Gieskes, W. W. C. *J. Biotechnol.* **1999**, *70*, 39.
2. Gültürk, E. A.; Güden, M.; Taşdemirci, A. *Compos B: Eng.* **2013**, *44*, 491.
3. Korunic, Z. *J. Stored Prod. Res.* **1998**, *34*, 87.
4. Yuan, P.; Liu, D.; Tan, D. Y.; Liu, K. K.; Yu, H. G.; Zhong, Y. H.; Yuan, A. H.; Yu, W. B.; He, H. P. *Microporous Mesoporous Mater.* **2013**, *170*, 9.
5. Fowler, C. E.; Buchber, C.; Lebeau, B.; Patarin, J.; Delacôte, C.; Walcarius, A. *Appl. Surf. Sci.* **2007**, *253*, 5485.
6. Puretskiy, N.; Chanda, J.; Stoychev, G.; Synytska, A.; Ionov, L. *Adv. Mater. Interfaces* **2015**, *2*, 1500124.
7. Round, F. E.; Crawford, R. M.; Mann, D. G. Diatoms: Biology and Morphology of the Genera; Cambridge University Press: Cambridge, UK, **2007**.
8. Jing, Y.; Jing, Z.; Ishida, E. H. *Ind. Eng. Chem. Res.* **2013**, *52*, 17865.
9. Aivalioti, M.; Papoulias, P.; Kousaiti, A.; Gidarakos, E. *J. Hazard. Mater.* **2012**, *207–208*, 117.
10. Rottman, J.; Platt, L. C.; Sierra-Alvarez, R.; Shadman, F. *Chem. Eng. J.* **2013**, *217*, 212.
11. van Garderen, N.; Clemens, F. J.; Kaufmann, J.; Urbanek, M.; Binkowski, M.; Graule, T.; Aneziris, C. G. *Microporous Mesoporous Mater.* **2012**, *151*, 255.
12. Ediz, N.; Bentli, İ.; Tatar, İ. *Int. J. Miner. Process.* **2010**, *94*, 129.
13. Losic, D.; Rosengarten, G.; Mitchell, J. G.; Voelcker, N. H. *J. Nanosci. Nanotechnol.* **2006**, *6*, 982.
14. Losic, D.; Triani, G.; Evans, P. J.; Atanacio, A.; Mitchell, J. G.; Voelcker, N. H. *Mater. Chem.* **2006**, *16*, 4029.
15. Posi, P.; Lertnimoolchai, S.; Sata, V.; Chindaprasirt, P. *Constr. Build. Mater.* **2013**, *47*, 896.
16. Oliveira, N. M.; Reis, R. L.; Mano, J. F. *ACS Appl. Mater. Interface.* **2013**, *5*, 4202.
17. Polizos, G.; Winter, K.; Lance, M. J.; Meyer, H. M.; Armstrong, B. L.; Schaeffer, D. A.; Simpson, J. T.; Hunter, S. R.; Datskos, P. G. *Appl. Surf. Sci.* **2014**, *292*, 563.
18. Nine, M. J.; Cole, M. A.; Johnson, L.; Tran, D. N. H.; Losic, D. *ACS Appl. Mater. Interface.* **2015**, *7*, 28482.
19. Bariana, M.; Aw, M. S.; Kurkuri, M.; Losic, D. *Int. J. Pharm.* **2013**, *443*, 230.
20. Vasani, R.; Losic, D.; Cavallaro, A.; Voelcker, N. *J. Mater. Chem. B* **2015**, *3*, 4325.

21. Milović, M.; Simović, S.; Lošić, D.; Dashevskiy, A.; Ibrić, S. *Eur. J. Pharm. Sci.* **2014**, *63*, 226.
22. Losic, D.; Yu, Y.; Aw, M. S.; Simovic, S.; Thierry, B.; Addai-Mensah, J. *Chem. Commun.* **2010**, *46*, 6323.
23. Crick, C. R.; Parkin, I. P. *Chem. Eur. J.* **2010**, *16*, 3568.
24. Erbil, H. Y.; Cansoy, C. E. *Langmuir* **2009**, *25*, 14135.
25. Yao, X.; Chen, Q.; Xu, L.; Li, Q.; Song, Y.; Gao, X.; Quéré, D.; Jiang, L. *Adv. Funct. Mater.* **2010**, *20*, 656.
26. Tourkine, P.; Le Merrer, M.; Quéré, D. *Langmuir* **2009**, *25*, 7214.
27. Furuta, T.; Sakai, M.; Isobe, T.; Nakajima, A. *Langmuir* **2010**, *26*, 13305.
28. Sakai, M.; Kono, H.; Nakajima, A.; Sakai, H.; Abe, M.; Fujishima, A. *Langmuir* **2009**, *26*, 1493.
29. Shibuichi, S.; Yamamoto, T.; Onda, T.; Tsujii, K. *J. Colloid Interface Sci.* **1998**, *208*, 287.
30. Tsujii, K.; Yamamoto, T.; Onda, T.; Shibuichi, S. *Angew. Chem. Int. Ed.* **1997**, *36*, 1011.
31. Onda, T.; Shibuichi, S.; Satoh, N.; Tsujii, K. *Langmuir* **1996**, *12*, 2125.
32. Shibuichi, S.; Onda, T.; Satoh, N.; Tsujii, K. *J. Phys. Chem.* **1996**, *100*, 19512.
33. Cao, L.; Jones, A. K.; Sikka, V. K.; Wu, J.; Gao, D. *Langmuir* **2009**, *25*, 12444.
34. Lai, Y.; Tang, Y.; Gong, J.; Gong, D.; Chi, L.; Lin, C.; Chen, Z. *Mater. Chem.* **2012**, 7420.
35. Shirtcliffe, N. J.; McHale, G.; Newton, M. I.; Zhang, Y. *ACS Appl. Mater. Interface.* **2009**, *1*, 1316.
36. Li, L.; Roethel, S.; Breedveld, V.; Hess, D. *Cellulose* **2013**, *20*, 3219.
37. Balu, B.; Breedveld, V.; Hess, D. W. *Langmuir* **2008**, *24*, 4785.
38. Teshima, K.; Sugimura, H.; Inoue, Y.; Takai, O.; Takano, A. *Appl. Surf. Sci.* **2005**, *244*, 619.
39. Nystrom, D.; Lindqvist, J.; Ostmark, E.; Hult, A.; Malmstrom, E. *Chem. Commun.* **2006**, 3594.
40. Chen, W.; Fadeev, A. Y.; Hsieh, M. C.; Öner, D.; Youngblood, J.; McCarthy, T. *J. Langmuir* **1999**, *15*, 3395.
41. Callies, M.; Chen, Y.; Marty, F.; Pépin, A.; Quéré, D. *Microelectron. Eng.* **2005**, *78–79*, 100.
42. Shirtcliffe, N. J.; McHale, G.; Newton, M. I.; Perry, C. C.; Roach, P. *Chem. Commun.* **2005**, 3135.
43. Simpson, J. T.; D'urso, B. R. Google Pat., **2012**.
44. Stalder, A. F.; Melchior, T.; Müller, M.; Sage, D.; Blu, T.; Unser, M. *Colloids Surf., A* **2010**, *364*, 72.
45. Rotenberg, Y.; Boruvka, L.; Neumann, A. W. *J. Colloid Interface Sci.* **1983**, *93*, 169.
46. Williams, D. L.; Kuhn, A. T.; Amann, M. A.; Hausinger, M. B.; Konarik, M. M.; Nesselrode, E. I. *Galvanotechnik* **2010**, *101*, 2502.
47. Lowell, S.; Shields, J. E. Powder Surface Area and Porosity; Springer: Netherlands, **1991**.
48. Seaton, N. A.; Walton, J. P. R. B.; Quirke, N. *Carbon* **1989**, *27*, 853.
49. Jo, H.; Blum, F. D. *Langmuir* **1999**, *15*, 2444.
50. Karmouch, R.; Ross, G. G. *Appl. Surf. Sci.* **2010**, *257*, 665.
51. Syakur, A.; Berahim, H. *Electr. Electron. Eng.* **2012**, *2*, 284.
52. Patel, A.; Patel, C.; Patel, M.; Patel, M.; Dighe, A. *Prog. Org. Coat.* **2010**, *67*, 255.
53. Makal, U.; Uslu, N.; Wynne, K. *J. Langmuir* **2007**, *23*, 209.
54. Al-Ghouti, M.; Khraisheh, M.; Allen, S.; Ahmad, M. *J. Environ. Manage.* **2003**, *69*, 229.
55. Pimraksa, K.; Chindaprasirt, P. *Ceramics Int.* **2009**, *35*, 471.
56. Yuan, P.; Yang, D.; Lin, Z.; He, H.; Wen, X.; Wang, L.; Deng, F. *J. Non-Cryst. Solids* **2006**, *352*, 3762.
57. Choi, M. C.; Sung, G.; Nagappan, S.; Han, M. J.; Ha, C. S. *J. Nanosci. Nanotechnol.* **2012**, *12*, 5788.
58. Pazokifard, S.; Mirabedini, S.; Esfandeh, M.; Farrokhpay, S. *Adv. Powder Technol.* **2012**, *23*, 428.
59. Dhôtel, A.; Li, H.; Fernandez-Ballester, L.; Delbreilh, L.; Youssef, B.; Zeng, X. C.; Tan, L. *J. Phys. Chem. C* **2011**, *115*, 10351.
60. Lee, H.; Owens, J. *J Mater. Sci.* **2010**, *45*, 3247.
61. Lin, Y.; Ehlert, G. J.; Bukowsky, C.; Sodano, H. A. *ACS Appl. Mater. Interfaces* **2011**, *3*, 2200.
62. Li, Y.; Huang, X. J.; Heo, S. H.; Li, C. C.; Choi, Y. K.; Cai, W. P.; Cho, S. O. *Langmuir* **2007**, *23*, 2169.
63. Shi, X.; Nguyen, T. A.; Suo, Z.; Wu, J.; Gong, J.; Avci, R. *Surf. Coat. Technol.* **2012**, *206*, 3700.
64. Nine, M. J.; Cole, M. A.; Johnson, L.; Tran, D. N.; Losic, D. *ACS Appl. Mater. Interface.* **2015**, *7*, 28482.
65. Lima, A. C.; Mano, J. F. *Nanomedicine* **2015**, *10*, 271.
66. Gordon, R.; Losic, D.; Tiffany, M. A.; Nagy, S. S.; Sterrenburg, F. A. *Trends Biotechnol.* **2009**, *27*, 116.